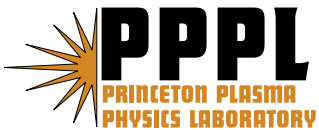


**On-axis Parallel Ion Speeds
near Mechanical and Magnetic Apertures
in a Helicon Plasma Device**

Xuan Sun, S.A Cohen,
Earl E. Scime, and Mahmood Miah

January 2006



Princeton Plasma Physics Laboratory

Report Disclaimers

Full Legal Disclaimer

This report was prepared as an account of work sponsored by an agency of the United States Government. Neither the United States Government nor any agency thereof, nor any of their employees, nor any of their contractors, subcontractors or their employees, makes any warranty, express or implied, or assumes any legal liability or responsibility for the accuracy, completeness, or any third party's use or the results of such use of any information, apparatus, product, or process disclosed, or represents that its use would not infringe privately owned rights. Reference herein to any specific commercial product, process, or service by trade name, trademark, manufacturer, or otherwise, does not necessarily constitute or imply its endorsement, recommendation, or favoring by the United States Government or any agency thereof or its contractors or subcontractors. The views and opinions of authors expressed herein do not necessarily state or reflect those of the United States Government or any agency thereof.

Trademark Disclaimer

Reference herein to any specific commercial product, process, or service by trade name, trademark, manufacturer, or otherwise, does not necessarily constitute or imply its endorsement, recommendation, or favoring by the United States Government or any agency thereof or its contractors or subcontractors.

PPPL Report Availability

Princeton Plasma Physics Laboratory

This report is posted on the U.S. Department of Energy's Princeton Plasma Physics Laboratory Publications and Reports web site in Fiscal Year 2006.

The home page for PPPL Reports and Publications is:

http://www.pppl.gov/pub_report/

Office of Scientific and Technical Information (OSTI):

Available electronically at: <http://www.osti.gov/bridge>.

Available for a processing fee to U.S. Department of Energy and its contractors, in paper from:

U.S. Department of Energy
Office of Scientific and Technical Information
P.O. Box 62
Oak Ridge, TN 37831-0062

Telephone: (865) 576-8401

Fax: (865) 576-5728

E-mail: reports@adonis.osti.gov

On-axis parallel ion speeds near mechanical and magnetic apertures in a helicon plasma device

Xuan Sun¹, S.A. Cohen², Earl E. Scime¹, and Mahmood Miah²

¹*Department of Physics, West Virginia University, Morgantown, West Virginia 26506*

²*Princeton Plasma Physics Laboratory, Princeton, New Jersey 08543*

Using laser-induced fluorescence, measurements of parallel ion velocities were made along the axis of a helicon-generated Ar plasma column whose radius was modified by spatially separated mechanical and magnetic apertures. Ion acceleration to supersonic speeds was observed 0.1-5 cm downstream of both aperture types, simultaneously generating two steady-state double layers (DLs) when both apertures were in place. The DL downstream of the mechanical aperture plate had a larger potential drop, $\Delta\phi_{\text{DL}} = 6-9kT_e$, compared to the DL downstream of the magnetic aperture, $\Delta\phi_{\text{DL}} \sim 3kT_e$. In the presheath region upstream of the mechanical aperture, the convective ion speed increased over a collisional distance from stagnant at 4 cm from the aperture to the 1.4 times the sound speed at the aperture. The dependence of the free- and trapped-ion-velocity-distribution functions on magnetic-field strength and mechanical-aperture electrical bias are also presented.

I. Introduction

Electrostatic double layers (DLs) in plasmas are isolated non-quasi-neutral regions remote from material surfaces.¹ Measured electric potential drops across DLs, $\Delta\phi_{\text{DL}}$, range from 3 to 30 kT_e/e and the DL length, typically 30 to 100 Debye lengths, λ_D , is much shorter than the electron-electron, ion-neutral, or ion-ion collision lengths. The resulting strong electric field in the collisionless plasma creates energetic particle beams. Usually,^{2,3} the ion-velocity-distribution function (IVDF) on the low-potential side of the DL contains the energetic beam and a low-energy ion population, the latter occurring because low-energy downstream ions decelerate if they approach the DL and are then reflected back downstream. The low-energy ion population on the low-potential side of the DL consists of a single Maxwellian distribution symmetric around the zero speed and is often called the “trapped” population in the literature. Ions, which originated on the high-potential side of the DL, accelerated through the DL, and formed the energetic beam on the low-potential side, are termed “free.” (Similar labels are applied to electrons on the high potential side.) The formation of DLs in laboratory plasmas may be promoted by a number of different means. The methods we employ use mechanical and magnetic apertures, both individually and in tandem.

A DL is frequently identified by measuring the spatial change of the plasma potential with Langmuir probes. Extracting, from probe data, the convective speed of ions or electrons transiting through or reflected by the DL is a difficult, and sometimes impossible, task. Retarding-field energy analyzers (RFEA) have been used with success to measure the free- and trapped-electron and ion energy distributions, though perturbations to the plasma occur with the RFEA inserted. (Perhaps nanotechnology will produce of an RFEA small enough to be non-perturbing.) Laser-induced fluorescence

(LIF) is a non-perturbing method to determine the velocity distribution of ions and atoms. There have been numerous LIF studies of ion flows in helicon plasma experiments.^{4,5,6} The results presented here are the first LIF measurements in helicon sources to provide detailed IVDFs upstream, in, and downstream of a DL for both trapped and free ions and with multiple DLs generated by tandem apertures.

Researchers using helicon plasma sources have reported the formation of current-free DLs at distances many helicon wavelengths from the helicon antennas. With Ar helicon plasmas generated at low pressure, < 0.5 mT, *Charles and Boswell*⁷ used an RFEA to study a DL with $\Delta\phi_{DL} = 3kT_e/e$ formed at the junction of their Pyrex helicon source and a metal expansion vessel. Both the potential profile and the energy of the ion beam accelerated through the DL were determined.⁸ In the same source, but for hydrogen plasmas, *Charles*⁹ also observed a supersonic ion beam, $2.1C_s$ (where $C_s = \sqrt{kT_e/M_i}$ and is the ion sound speed), and attributed the beam to the presence of a double layer. Using a tunable diode-laser-based laser-induced-fluorescence diagnostic,¹⁰ *Cohen, et al.* reported supersonic velocities of argon ions which had passed through a mechanical aperture located 1-cm upstream of a region of converging-diverging magnetic-field, termed a magnetic nozzle or a magnetic aperture. Supersonic flows were only detected under conditions of high-helicon-axial-power-flow (> 30 W/cm²) and low-ambient-gas pressure (< 1.5 mT) in the helicon source. These helicon plasmas had peak parameters in the range $n_e = 1-5 \times 10^{13}$ cm⁻³ and $T_e = 3-8$ eV. The abundance of metastable Ar ions – those detectable by LIF – flowing at supersonic speeds in the magnetic-field expansion region (ER) decreased exponentially as the neutral pressure in the expansion region, P_{ER} , increased. In the center of the helicon source chamber, about 30 cm upstream of aperture plate and 30 cm downstream of the helicon antenna, ions

were stagnant, *i.e.*, their flow speed was below the ion thermal speed. The rapid acceleration of ions as they passed through the aperture was the evidence that a DL existed in the nozzle region. Limited optical viewing access did not permit LIF measurements near the magnetic-nozzle midplane. Also using an LIF system, *Sun, et al.* reported that at ~ 1 m from the antenna in a low-axial-power-flow (~ 5 W/cm²), large-radius, low-neutral-pressure helicon argon plasma source, a supersonic ion beam developed where the plasma exited the source chamber into an expansion chamber. In addition to the ion beam, a cold, subsonically drifting background ion population was observed.

Features common to these and several earlier non-helicon DL-producing experiments are apertures – mechanical or magnetic – and low neutral-gas pressures. Neutral-gas pressure affects both plasma diagnostics (especially Ar^{+*} LIF) and plasma parameters such as collisionality, hence the IVDF, the ionization source, and the pre-sheath length. These pressure-related topics will be discussed in a later work. Herein we confine our attention to apertures as they affect IVDFs and DLs. We also restrict attention to on-axis ion flows. Future work should probe off-axis flows, addressing questions on reverse flows, return currents, and radial expansion.

In the context of the physics of double layers, what is an aperture? An aperture (in a plate) is a hole of radius, r_a , smaller than the plasma column's radius, r_p , which divides the plasma column into source and expansion regions, see Figure 1. Apertures reduce neutral-gas flow between the plasma source and the plasma expansion regions. We discount the primacy of this effect – certainly at low pressure, < 2 mT – since we have seen DLs with equal and unequal gas pressures in both regions. Apertures also separate the region of energy input *via* the helicon wave, the main (or source) chamber, from the

expansion region, where the energy input is in the form of particle enthalpy. This has a profound effect on particle creation rate. Apertures may alter the ratio of ion to electron fluxes from the source region into the ER, in part due to differing gyro-radii. (The large gyroradii of ions ($\rho_i \sim 0.1$ to 1 cm) compared to electrons ($\rho_e \sim 4 \times 10^{-3}$ to 4×10^{-2} cm) in our experiment will also change the radial distribution of ions and electrons on the downstream side of the DL. The strongest effect on particle fluxes arises from the self-consistent electric field, whose value is set by Poisson's equation. Differing particle mobilities enter the momentum and energy equations.

Mechanical aperture plates establish an equipotential boundary in a plane around the aperture hole and on the surfaces surrounding the hole. In the experiments described here, the short sheath thickness, $s\lambda_D < 10^{-3}$ cm, in the source chamber results in a strong electric field at the aperture plate's surface, $> 10^4$ V/cm. The presheath with a characteristic length ~ 3 cm, much larger than the aperture diameter, can create a nearly flat equipotential across the upstream side of the aperture hole.¹¹

A magnetic aperture is a region of converging/diverging magnetic field, sometimes called a magnetic Laval nozzle. The basic idea is to compress the plasma by shrinking the cross section of magnetic flux tubes and then, as the plasma enters the expanding section of the nozzle magnetic field, supersonic ion speeds are achieved by converting the thermal (random) energy into directed (flow) energy. Magnetic Laval nozzles were used to create a supersonic ion beam in a plasma in 1969. Mach numbers as large as 3 were obtained in Q-machine.¹² More recently, a magnetic nozzle has been proposed for the VASIMR rocket to convert thermal energy into thrust.^{13, 14} Note that, in the measurements reported here and earlier, the ion beam energy decreased with increasing nozzle field strength. Therefore, the ion acceleration to supersonic speeds is

not simply understood by the analogy to the mechanical Laval nozzle. Efforts must be made to understand the static electric field, *i.e.*, the DL, which creates the energetic ion beam. Even for a purely divergent magnetic field configuration (no compression region), *Sun, et al.* observed supersonic ion flow speed which increased with decreasing magnetic-field strength in the expansion region.

That static electric double layers can form in a current-free plasma expanding in a divergent magnetic field was predicted in an analytical study by *Perkins and Sun* in 1981.¹⁵ Although they predicted a stable DL required $T_e < T_i$, there is strong experimental evidence that stable DLs can exist in expanding plasmas with $T_e > T_i$ in the absence or presence¹⁶ of current. More recently, a one-dimensional, hybrid simulation (particle ions and fluid electrons) that modeled rapid plasma expansion in a diverging magnetic field with an axial-position-dependent electron loss rate in a uniform magnetic field showed that the rapid decrease in plasma density, such as due to a diverging magnetic field, is consistent with double-layer formation in a current-free plasma.¹⁷ In that simulation, a short ($\sim 7 \lambda_D$) 14 eV DL formed at the location of rapid plasma expansion for upstream parameters of 0.5 mTorr, $n_e = 6.5 \times 10^8 \text{ cm}^{-3}$ and $T_e = 7.2 \text{ eV}$. Throughout the simulation volume, a low-energy population of ions, corresponding to ions created by ionization and by charge-exchange collisions, was observed. Downstream of the DL, a high-energy ion population, corresponding to ions accelerated through the DL potential drop, was observed in addition to the low-energy background population. The total ion acceleration occurred over roughly an ion mean free path.

A recent experiment by *Plihon et al.* confirmed DL formation in an axially uniform plasma with a uniform magnetic field and a strong axial density gradient.¹⁸ By puffing SF₆ gas into the plasma at a single axial location, the highly electronegative SF₆

gas created a strong electron density gradient along the plasma axis by substantially reducing the electron density - thereby simulating rapid plasma expansion without a divergent magnetic field.

To the best of our knowledge, no computational study of the effects of overall magnetic field strength on DLs is available in the literature. As will be shown by these experiments, there is a clear correlation between the strength of the magnetic field, the magnitude of the potential drop across the DL, and the floating potential of an aperture placed in the plasma. The large floating potentials of the aperture is suggestive of the presence of energetic electrons in the helicon plasma. Whether such suprathermal electrons exist in helicon plasma devices is still a hotly debated issue in the helicon source community. Since a small population, $\sim 10\%$, of energetic electrons in a cooler background plasma has been shown to induce the formation of a free-standing current-free double layer,¹⁹ the DL measurements presented in this work may also shed light on the question of energetic electrons in helicon plasmas. Other experiments demonstrated that smaller energetic populations, as low as 1% of the bulk, are sufficient to sustain a DL and that the DL strength increased with the number of energetic electrons.²⁰

There are also other questions concerning the role of an aperture in a plasma. For example, will the presheath electric field be affected if an aperture is created in an absorbing wall? *Riemann* argued that the length of presheath should be equal to the ion-neutral collision length in his model of plasma sheaths.²¹ *Oksuz* and *Hershkowitz* verified *Riemann's* presheath model experimentally on a surface immersed in a low density, low temperature, weakly collisional, argon plasma.²² They found that the potential drop across the presheath is $\Delta\phi_{ps} \sim kT_e/e$, instead of $kT_e/2e$ as determined in the *Riemann* sheath model. The experimental data that will be presented in this work show that the

potential drop is $\sim kT_e/e$ in front of an aperture in a metal plate. The role of a small superthermal electron population in setting $\Delta\phi_{ps}$ as well as $\Delta\phi_{DL}$ cannot be discounted.²³ We also have installed two apertures, separated by up to $10^5 \lambda_D$, to explore whether the strongly modified (upstream) IVDF and EEDF will promote formation of a second DL at the second aperture.

With a tunable diode-laser-based LIF diagnostic, we have mapped the argon-IVDF on the high- and low-potential sides of a DL localized beyond an aperture in a metal plate located many wavelengths from the helicon source. The strength and spatial extent of the DL was determined from measurements of the spatial dependence of the free-ion energy downstream of the DL. The effect of the location of the aperture plate -- relative to the magnetic field coils -- on the DL was investigated by re-positioning the aperture plate to the following locations: 1) the center of the main chamber; 2) the magnetic nozzle region at the end of main chamber; and 3) the expansion region downstream of the magnetic nozzle coil. Without any aperture plate, the IVDF measurements show that a 20 V potential drop develops over a distance of 3 cm, $\sim 500 \lambda_D$, beyond the 2-cm ID magnetic nozzle at the end of main chamber. (The nozzle coil acts as both a mechanical and a magnetic aperture.) With a mechanical aperture plate also placed in the plasma, an additional DL forms. Short regions, ~ 0.5 cm, of free-ion deceleration in the DL and also backflowing (reflected or trapped) cold ions have been observed, indicating that the DL is of the ion-acoustic type. Ion acceleration in the presheath was also measured by the LIF.

II. Experimental Apparatus

The experiments were performed in the Magnetic-Nozzle-eXperiment (MNX) facility (see Fig. 1). A 4-cm diameter, steady-state helicon plasma flows along the magnetic field formed by a Helmholtz-coil pair. The plasma exits the source (or main) chamber through a coaxial 2-cm-i.d., 3-cm-long nozzle coil used to control the magnetic field gradient. The nozzle coil extends from $z = -1.5$ cm to $z = 1.5$ cm. Figure 1 (b) shows the axial field strength near the nozzle at a Helmholtz coil current of 50 A and nozzle current of 400 A, typical of experimental conditions in this paper. Exiting the nozzle coil, the plasma enters a 10-cm-i.d., 100-cm-long Pyrex tube termed the expansion region (ER). The ER has 15 internal 4-cm-i.d. coaxial copper rings, of which eight may be electrically biased. The floating potentials of the copper rings in the ER were typically -40 to -120 V. Such large floating potentials suggest the presence of energetic electrons in the ER. Floating potentials in the main chamber are much lower, ~ -30 Volts, indicating that an energetic electron population, if present, has a population less than $(m_e/M_{Ar})^{1/2} \sim 1/300$ smaller than that of the bulk electrons.^{24, 25}

Also shown in Fig. 1(a) are three electrically biasable metal disks, labeled *endplate*, *M2*, and *M3*. For the experiments reported here, the endplate and *M3* were electrically floating. The disk *M2*, i.e., the aperture plate, has a hole, the aperture, which limits the plasma and neutral gas flows and helicon-wave propagation into the ER. Fig. 2 shows five locations where *M2* may be positioned. Also, *M2* may be completely removed, as shown in Fig. 2a). (The aperture diameters and plate thicknesses are indicated on the figure.) Sheaths of differing thickness will form on opposite sides of the aperture plate, predominantly because of the different plasma densities on the two sides of the plate. Based on Langmuir probe measurements at the center of the main chamber and in the expansion chamber 10 cm from the aperture, the ratio of the Debye lengths in the ER to

that in the source chamber is $\lambda_{D/ER}/\lambda_{D/S}$ is ~ 10 , with $\lambda_{D/S} \sim 6 \times 10^{-4}$ cm. Control of pumping speed in the ER allows the ratio of ion-neutral collision lengths to be varied, $0.1 < \lambda_{ER}/\lambda_{in/S} < 10$, with $1 < \lambda_{in/S} < 10$ cm.

For LIF measurements, the laser is directed down the axis of the plasma column, through the entire expansion region (ER) and main chamber into the helicon antenna region and onto the end plate. Before entering the MNX vacuum chamber, the laser is sent through a quarter-wave plate, allowing creation of either right or left circularly polarized light for exciting either the σ^- or σ^+ transitions in Ar^{*+} . The shift in the center wavelength of the measured LIF signal is used to determine the average flow of the ions along the laser path. A detailed description of LIF measurement principles can be found in Ref. 11.

III. Experimental Results and Discussion

A. The magnetic nozzle as an aperture

Without an aperture plate, Fig. 2a, the plasma flows into the expansion region from the main chamber through the 2-cm-i.d. of the magnetic-nozzle coil. The midplane of the nozzle coil is defined as $z = 0$ cm. Figure 3 shows the flow speed at $z = -3.0$ cm in the ER versus the nozzle-magnetic-field strength for an rf-power of 800 Watts, magnetic field (B_H) of 580 Gauss at the center of the source chamber, and neutral pressures of 0.7 mTorr and 0.2 mTorr in source (P_M) chamber and ER (P_{ER}), respectively. The energy of the exiting ion beam decreases with increasing nozzle field strength until the (added) nozzle field strength reaches 2000 Gauss. (At $B_n = 2000$ G, the ratio, R , between the on-axis magnetic field at the nozzle midplane to that in the center of the ER was $R = 4.75$. At $R = 4$, a 4-cm-dia plasma column will pass through the nozzle without contacting the

nozzle coil housing.) The ion beam energy at $z = -3.0$ cm is approximately 7 eV for $B_N = 2000$ G. The corresponding Mach number (V/C_s) was ~ 1.3 . For nozzle magnetic field strengths below 1000 Gauss, the LIF signal was too weak to give a good measure of ion speed.

Our earlier published data at higher B_H fields of 1200 G and with a mechanical aperture located in front of the magnetic nozzle coil, as in fig. 2b), Ref. 6, showed qualitatively similar behavior, i.e., a 5% decrease in ion energy, E_i , with increasing B_n , for $0 < B_n < 2000$ G, but E_i rising 3% for $2000 \text{ G} < B_n < 3000$ G. Those earlier results showed considerably higher flow energies ($E_i \sim 18$ eV) and speeds, $M \sim 1.7$ at $z = -2$ cm. At these lower B_H values, $R < 4$ at $B_n = 2000$ G, the effect of the nozzle magnetic field is qualitatively similar to that of a purely magnetic aperture.

B. Mechanical aperture plate

By placing the aperture plate (AP) at four different positions relative to the mid-plane of the magnetic-nozzle coil, we investigated the effect of aperture-plate location on the parallel ion flow speed. A 0.1 eV argon ion would have a gyroradius of 0.1-1 cm (5000-500 G), comparable to the radii of the various apertures used, 0.25-0.4 cm. The transit time for ions, accelerated by the presheath to 5 eV, to pass through the thin aperture plate is 2-20 times shorter than the ion gyroperiod. Independent of aperture plate installation, the ion flow speed (energy) in the center of the main chamber is very small, less than 0.03 eV. The perpendicular ion temperature is slightly higher, ~ 0.05 -0.5 eV. Thus, ions pass through the aperture on nearly straight lines, within 30° of the plate normal.

B.1 Aperture plate immediately upstream of nozzle coil

With the AP positioned as shown in Fig. 2b, just upstream of the AP, at $z = -2.3$ cm, the ion flow energy increases to 1.1 eV (Fig. 4). After the AP and nozzle region, the ion flow energy increases further to 13.0 eV at $z = 2.4$ cm. By $z = 7.4$ cm, the ion beam energy is up to 17.7 eV. Coexistent with the ion beam is a low-energy population in the ER. Throughout this paper we use terminology introduced in Ref. 6: high energy particles are called HEP; low energy particles are called LEP. The LEP, represented by the diamond symbols in Fig. 4, has zero net flow throughout the expansion region. The lack of LEP net flow persists even in the DL where the HEP ions accelerate from 7800 m/s (12.7 eV) to 9200 m/s (17.6 eV) in 4.6 cm. These observations are consistent LIF-measured IVDFs in other helicon DL experiments.²⁶

Although the LEP ion peak was generally stagnant (as shown later in Fig.7) or had slightly positive speeds (as shown in Fig. 4), significant LEP ion flows in the $-z$ direction were observed with higher rf power (950 Watts) and lower neutral pressure (0.4 mTorr), as shown in Fig. 5. Locations distant from the nozzle, e.g., at $z = 8.7$ cm, showed a single Maxwellian with no axial flow. Locations closer to the nozzle showed increasing flow back towards the nozzle, which suggest a modest negative potential dip occurs downstream of the DL. The depth of the potential dip is at least 0.2 V, or about a hundredth of DL potential drop. Such a dip is characteristic of an ion-acoustic DL.²⁷

Fig. 6 shows the ion-beam energy measured at $z = 3.2$ cm and the current collected by the aperture plate *versus* a bias voltage applied to the AP. The minimum ion beam energy occurs at a bias voltage of 9.1 V (close to the measured plasma potential of 9.8 ± 1.0 V). When the AP is biased more negative than the plasma potential, the ion beam energy increases until the bias voltage equals the floating potential. Further

decreases in applied bias potential lower the ion beam energy slightly. At the negative potentials, -30 to -70 V, the AP collects ion saturation current. A bias voltage above the plasma potential, from 10 to 30 V, also increases the ion-beam energy. Electron saturation current to the AP is not achievable with the current and voltage capabilities of the AP biasing power supply and instability of the plasma column.

For an expanding, two-electron-temperature plasma terminated with a metal plate at one end, Hairapetian and Stenzel reported that the DL amplitude decreased as an increasing positive bias voltage was applied to the end plate.^{20,28} They reported that the DL disappeared at large positive bias voltage and that negative bias voltages had no effect on their DL. Consistent with their results, a large negative bias voltage had little effect on the ion beam energy in these experiments. However, the detailed LIF measurements indicate that the ion beam energy does decrease slightly with negative bias until the bias AP enters ion saturation – suggesting a slight weakening of the DL until the maximum ion current is pulled through the sheath onto the AP. Similarly, and consistent with the Hairapetian and Stenzel observations, the ion beam energy also decreases with increasing positive AP bias voltage until the bias voltage equal to 9.1 V or close to the plasma potential (9.8 V). We hypothesize that increasing the electron current into the DL (through the positive bias voltage), increases the ratio of thermal to energetic electron densities – thereby decreasing the strength of the DL.^{20,28} In contrast to the Hairapetian and Stenzel results, at large positive bias voltages (when the AP enters into electron saturation, or for bias voltages larger than the plasma potential) the ion beam energy returns to the same level as when the AP was biased at the negative potential.

B.2 Aperture plate near center of the source chamber

With the AP inserted into the plasma near the nozzle coil, the parallel ion kinetic energy at $z = 3.0$ cm increased from 9 eV (Fig. 3) to 14 eV (Fig. 4). To better understand the effect of the AP, we separated the AP (mechanical aperture) and nozzle (magnetic aperture) by positioning the AP near the center of the source (main) chamber, between -29.1 and -29.4 cm, see Fig. 2d). The viewing geometry in this configuration allowed spatially resolved measurement of parallel ion flow speeds around both the mechanical and magnetic apertures. As shown in Fig. 7, ions begin to accelerate at $z = -31.4$ cm and enter the aperture hole with an energy of 7.2 eV at $z = -29.4$ cm (Fig. 7). The ions keep accelerating as they transit the aperture and reach 20.4 eV at $z = -28.9$ cm (Fig. 7). Further downstream of the AP, at $z = -28.1$ cm, the ions reached 39.5 eV $\sim 7 T_e$. Thus, the ions accelerated from 7.2 eV to 39.5 eV in 1.2 cm, $\sim 2000 s\lambda_D$ or $\sim 200 ER\lambda_D$.

In the expansion region beyond the nozzle coil ($z > 1$ cm), three ion populations are observed, see Fig. 7. The LEP ions with parallel kinetic energy ~ 0.1 eV are produced locally in the expansion region. We suggest that the ions with kinetic energy ~ 16.3 eV at $z = 4.4$ cm (~ 7 eV at $z = 3$ cm, as shown in Fig. 7) were created in the region between the AP and the nozzle coil and then accelerated through a DL at the nozzle, gaining ~ 16 eV in transit. A third, super-high-energy, population (SHEP) is observed downstream of the nozzle ($z = 2.9$ cm) having a flow energy of 51 eV. The 51 eV energy is consistent with the observation of a roughly 40 eV energy increase at the AP followed by a 7-10 eV increase at the magnetic nozzle at $z = 2.9$ cm. In other words, this configuration of a mechanical AP followed by magnetic nozzle leads to the formation of two distinct double layers.

Since a DL is essentially a plasma sheath that forms in the interior of a plasma, a

presheath must arise to match the plasma potential to that of the DL.²⁹ To satisfy the Bohm Criterion for ions falling into the sheath at the edge of the DL, the ions must reach a minimum parallel energy of $\frac{1}{2} kT_e$ by passing through the presheath. The measured ion acceleration before the DL is shown in Fig. 8 for the AP placed at $z = -29.4$ cm. The ions begin to accelerate ~ 3 cm before the plate, approximately equal to the expected length of the presheath, the ion-neutral collision length.^{21,22} The beam energies at the aperture are 6.7 eV, 7.2 eV, and 8.3 eV for 500, 800, and 1100 Watts of RF power. Langmuir probe measurements at $z \approx -32 \pm 0.15$ cm indicate that the electron temperatures are 8.0 ± 1.0 eV, 8.4 ± 1.0 eV, and 8.4 ± 1.0 eV. Langmuir probe characteristics show an energetic electron population, if at all present, had a density less than 0.1% of the bulk electrons. Thus, the ion energies at the aperture indicate a kT_e/e potential drop in transiting the presheath. The presheath region, as indicated in Fig.8, is 4-5 cm, which, as noted before is approximately equal to the ion-neutral mean-free-path of 3-5 cm. Thus, the thickness of the presheath is consistent with Riemann's sheath model. However, similar to *Oksuz* and *Hershkowitz's* experiment, the potential drop over the presheath is $\sim T_e/e$, instead of $kT_e/2e$ in Riemann's model. The exiting ion flow energies at $z = -27.6$ cm, about 1.5 cm from the exit of aperture, are 36.5, 39.6, and 47.8 eV for these three RF power scan, *i.e.* the strength of sheath DL increases with increasing rf power.

Note that although the plasma parameters upstream of nozzle are dramatically different in Fig.4 and Fig.7, the strength of DLs formed by the nozzle magnetic field are nearly identical, about 20 V or $\sim 3kT_e/e$. Although no spatial scan was performed for the configuration without an aperture plate, the increase in ion kinetic energy close to the magnetic aperture is approximately the same, 7.0 eV at $z = 3.0$ cm with $B_N = 2250$ G, for configurations 2a and 2d. Thus, these measurements suggest that the nozzle magnetic

field creates an overall 20 V potential drop along the axis even though the detailed DL structure does depend on the upstream plasma parameters (as indicated by Fig. 4 and Fig. 7).

B.3 Aperture plate in the expansion chamber

The floating potential achieved by an electrically floating AP placed in the expansion region of the experiment is indicative of a density-weighted average energy of the electron population in the plasma. Shown in Fig. 9 are measurements of the z-directed ion energy at $z = 5.3$ cm for the AP at $z = 4.5$ cm (the AP position as indicated in Fig. 2e) and the aperture-plate floating potential *versus* nozzle magnetic field strength. Both the ion flow energy and the floating potential of the AP increase with decreasing nozzle magnetic field strength. The large negative floating potential, up to -75 V, of the electrically isolated aperture plate in the expansion chamber suggests the existence of energetic electrons in the plasma. The existence of energetic electrons in helicon sources, possibly resulting from Landau damping of the helicon wave, has long been debated amongst the helicon source community.³⁰ Reports of energetic electrons in long, low axial-power density, higher neutral pressure helicon plasmas indicated that the energetic population was less than $\sim 10^{-4}$ of the bulk, thus the Landau damping explanation for the high ionization efficiency of helicon sources has fallen into some disfavor.^{31,32} However, the LIF measurements presented here, for a relatively short, higher power-density device, indicate a strong correlation between the mechanism responsible for determining the strength of the DL and the floating potential of the AP – possibly a result of DL formation being controlled by a population of energetic electrons in the helicon source.

If the high floating potential of the AP results from an energetic electron population, the same population of energetic electrons should determine the strength of the ion-accelerating DL and both the AP floating potential and the ion beam energy will have similar dependencies on the source parameters.²⁰ Note also that if the higher nozzle field strength results in more energetic electrons reflected back into source, i.e. fewer energetic electrons can reach the AP downstream of nozzle, the decrease in the strength of the DL and the decrease in the AP floating potential with increasing nozzle magnetic field strength are easily explained. Typically it is expected that an increasing magnetic nozzle field strength leads to higher energy ion beams. These results indicate that if the ion beam is created in a DL at a magnetic nozzle, a weaker nozzle magnetic field that does a poorer job of confining the energetic source electrons is more effective at ion beam creation and acceleration.

3. Summary

In summary, detailed measurements were made of the velocity distribution of free and trapped ions in the vicinity of single and multiple double layer structures. Near and in the DL the trapped ion velocity distribution is well represented by a single, nearly stationary Maxwellian velocity distribution. The measured free ion speeds reveal the DL formed by nozzle is about $3kT_e/e$, independent of the upstream IVDF and EEDF. Acceleration of ions up to -- and exceeding -- the ion sound speed (determined by the bulk electron temperature) is observed in the presheath upstream of the DL. The potential drop over the presheath is $\sim kT_e/e$.

Multiple double-layer structures were produced by first creating a DL at an electrically floating plate placed in the plasma source chamber. Then, the plasma

downstream of the first DL flowed through a second DL created by a rapid plasma expansion in the divergent magnetic field of a magnetic nozzle coil. That a mechanical aperture can create a DL with strength $\sim 6kT_e/e$ and thereby increase the exit velocity of ions flowing through an additional DL further downstream suggests that a sequence of appropriately sized apertures could be used to increase the specific impulse of plasma thrusters or other systems used to create ion beams.

Perhaps the most significant result from this work is that for expanding helicon source plasmas the ion beams created by the DL in a magnetic aperture appear to depend on the energetic electron population that can escape the source region. Therefore, as seen in other experiments, configurations with no nozzle magnetic field and very weak fields in the expansion region yield the highest energy ion beams. Recent investigations by comparing different spectroscopic line ratios also suggest the existence of a small population ($\sim 0.1\%$) of suprathermal electrons ($\sim 10kT_e$).³³

Further studies are still needed to explore the relationship between DL strength and aperture size, the dependence of the threshold pressure for DL formation on gas species and neutral gas temperature, and the effects of multiple gas species on the strength of the DL.

Acknowledgments

This work was supported, in part, by U.S. Department of Energy Contract No. DE-AC02-76-CHO-3073 and NSF grant PHY-0315356. We thank Bruce Berlinger for excellent technical support.

References

- ¹ M.A. Raadu, Physics Reports **178**, 25 (1989) and references therein.
- ² L. R. Block, Astrophys. Space Sci. **55**,59 (1978)
- ³ B. H. Quon, and A. Y. Wong, Phys. Rev. Lett. **37**,1393 (1976)
- ⁴ E. E. Scime, P. A. Keiter, S. P. Gary, M. Balkey, R. F. Boivin, J. L. Kline, and M. Blackburn, Phys. Plasmas **7**, 2157 (2000).
- ⁵ X. Sun, C. Biloiu, R. Hardin, and E. E. Scime, Plasma Source Sci. Technol. **13** 359 (2004)
- ⁶ S. A. Cohen, N. S. Siefert, S. Stange, R. F. Boivin, E. E. Scime, and F. M. Levinton, Phys. Plasmas **7**, 2593 (2003)
- ⁷ C. Charles, and R. W. Boswell, Appl. Phys. Lett. **82**, 1356 (2003)
- ⁸ C. Charles, A. W. Degeling, T. E. Sheridan, J. H. Harris, M. A. Lieberman, and R. W. Boswell, Phys. Plasmas **7**, 5232 (2000).
- ⁹ C. Charles, Appl. Phys. Lett. **84**, 332 (2004)
- ¹⁰ R. F. Boivin, and E. E. Scime, Rev. Sci. Instrum. **74**, 4352 (2003)
- ¹¹ P. C. Stangeby, Plasma Sheath in Physics of Plasma-Wall Interactions in Controlled Fusion Devices (Plenum Press, 1984)
- ¹² S. A. Andersen, V.O. Jensen, P. Nielsen, and N.D' Angelo, Phys. Fluids **12**, 557 (1969)
- ¹³ A. V. Arefiev, and B. N. Breizman, Phys. Plasmas **11**, 2942 (2004)
- ¹⁴ F. Chang-Diaz, Sci. Am. **283**, 90 (2002).
- ¹⁵ F. W. Perkins and Y.C. Sun, Phys. Rev. Lett. **46** 115 (1981).
- ¹⁶ R. Schrittwieser, I. Axnas, T. Carpenter, and S. Torven, IEEE Trans. on Plasma Sci., **20**, 607 (1992).
- ¹⁷ A. Meige, R. W. Boswell, C. Charles, and M. M. Tuner, Phys. Plasmas **12**, 052317 (2005).
- ¹⁸ N. Plihon, C. S. Corr, and P. Chabert, Appl. Phys. Lett. **86**, 091501 (2005).
- ¹⁹ K. Sato, and F. Miyawaki, Phys. Fluids B **4**, 1247 (1992)
- ²⁰ G. Hairapetian, and R. Stenzel, Phys. Fluids B **3**, 899 (1991)
- ²¹ K.U. Riemann, Phys. Plasmas **4**, 4158 (1997)

- ²² L. Oksuz, and N. Hershkowitz, Phys. Rev. Lett. **89**, 145001 (2002)
- ²³ R.W. Boswell, A.J. Lichtenberg and D. Vender, IEEE Trans. Plasma Sci **20**, 62 (1992)
- ²⁴ K. Shiraishi and S. Takamura, J. Nucl Mater. **176-177**, 251 (1990)
- ²⁵ M. Cercek and T. Gyergyek J. Phys. D **34**, 330 (2001)
- ²⁶ X. Sun, A. M. Keesee, C. Biloiu, E. E. Scime, A. Meige, C. Charles, and R. W. Boswell, Phy. Rev. Lett. **95**, 025004 (2005)
- ²⁷ N. Hershkowitz, Space Science Rev. **41**, 351 (1985)
- ²⁸ G. Hairapetian, and R. Stenzel, Phys. Rev. Lett. **65**, 175 (1990)
- ²⁹ N. Hershkowitz, IEEE Trans. on Plasma Sci. **22**, 11 (1994)
- ³⁰ F. F. Chen, Plasma Phys. Controlled Fusion **33**, 339 (1991)
- ³¹ A. W. Molvik, T. D. Rognlien, J. A. Byers, R. H. Cohen, A. R. Ellingboe, E. B. Hooper, H. S. McLean, B. W. Stallard, and P. A. Vitello, J. Vac. Sci. Technol. A **14**, 984 (1996)
- ³² F. F. Chen, and D. D. Blackwell, Phys. Rev. Lett. **82**, 2677 (1999)
- ³³ S. A. Cohen, X. Sun, N. M. Ferraro, E. E. Scime, M. Miah, S. Stange, N. Siefert, and R. Boivin, submitted to IEEE Trans. Plasma Sci. (2005)

Figure Captions:

Fig. 1 (a) The schematic of the Magnetic Nozzle experiment (MNX). Argon plasma is formed by absorption of helicon waves launched from a double-saddle antenna. The plasma flows through the main chamber along magnetic field lines created by a set of Helmholtz coils. The plasma then flows through metal aperture M2 and the nozzle coil into the expansion region (ER). The beam of a diode laser is directed along the MNX axis, allowing LIF measurements throughout MNX. (b) Scanning mechanism for the LIF collection optics allows 12 lines-of-sight (LOS) intercepting axial points in the ER near the nozzle. (c) The axial field strength near the nozzle at a Helmholtz coil current of 50 A and a nozzle current of 400 A, typical of experimental conditions in this paper.

Fig. 2 Five different configurations were used the experiments: (a) without aperture plate and the measurement were performed in the ER; (b) a metal disk with an aperture of 0.48 cm and thickness of 0.305 cm was placed immediately before the nozzle. The measurements were performed in both the ER and source. (measurements performed with the 0.8-cm-aperture are not presented here); (c) the aperture used in (b) was moved 1.9 cm into source (data for this configuration are not reported in this paper); (d) the aperture used in (b) was moved 27.6 cm into the source and measurements were performed near the aperture plate and in the ER; (e) a metal disk with an aperture of 0.48 cm and thickness of 0.165 cm was placed in the ER. The measurements were performed near the aperture plate.

Fig. 3 The beam energy versus the nozzle field strength at $z = 3.0$ cm for RF power of 800 W, $B_H = 580$ G, $P_M = 0.7$ mTorr, $P_{ER} = 0.2$ mTorr, and no aperture plate (M2).

Fig. 4 The beam energy versus z for AP at $z = -1.8$ cm and plasma conditions of rf power $P = 600-900$ W; $B_H = 580$ G; $B_N = 2250$ G; $P_M = 0.6$ mTorr; $P_{ER} = 0.3-0.7$ mTorr. The open diamonds label ions created locally in the EP (the LEP). The open circles label ions in and emanating from the source (which become HEP ions in the ER).

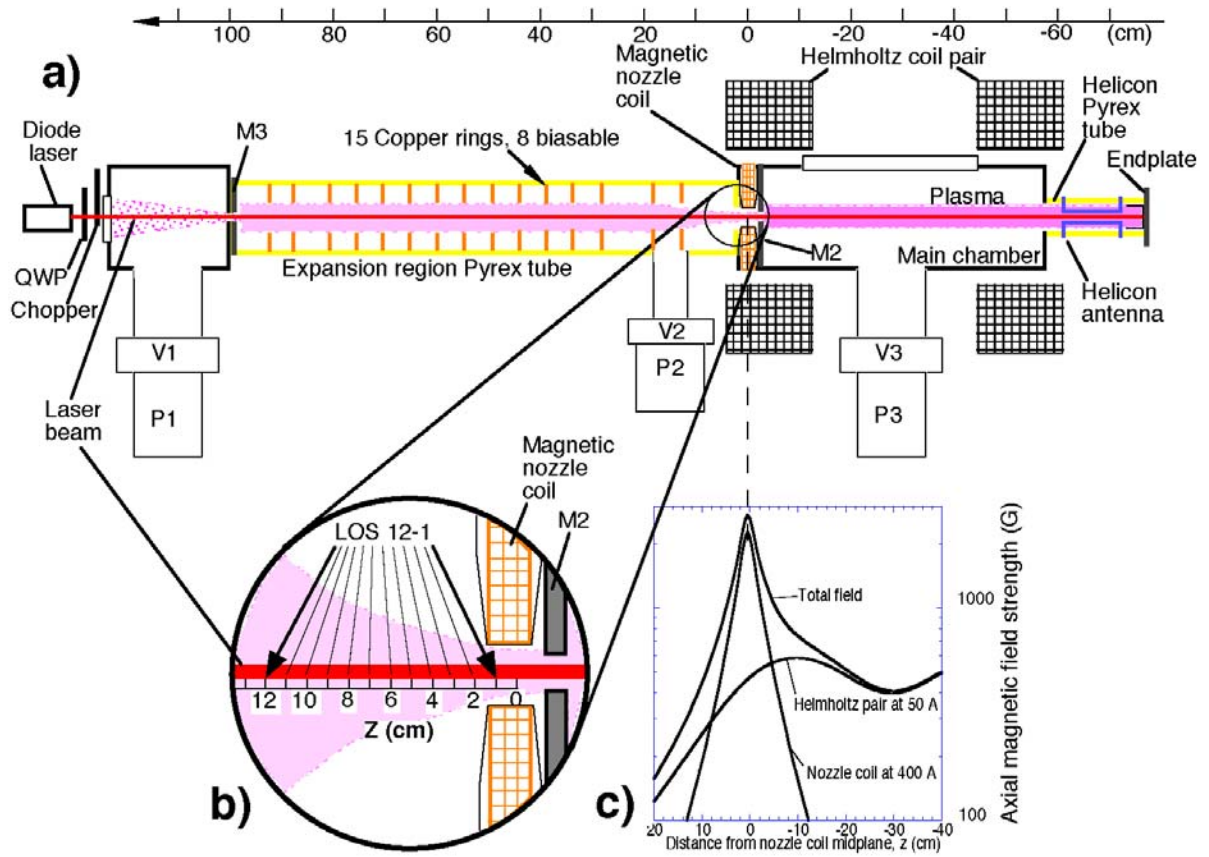
Fig. 5: Example of reversed flow of LEP ion population at various axial positions. Negative speeds indicate ions moving upstream towards the source.

Fig. 6: The ion beam energy versus the bias voltage on the aperture plate at $z = -3.2$ cm for rf power of 700-800 W, $B_H = 580$ G, $B_N = 1700$ G, $P_M = 0.7$ mTorr, and $P_{ER} = 0.3$ mTorr. The aperture plate was at $z = -1.8$ cm.

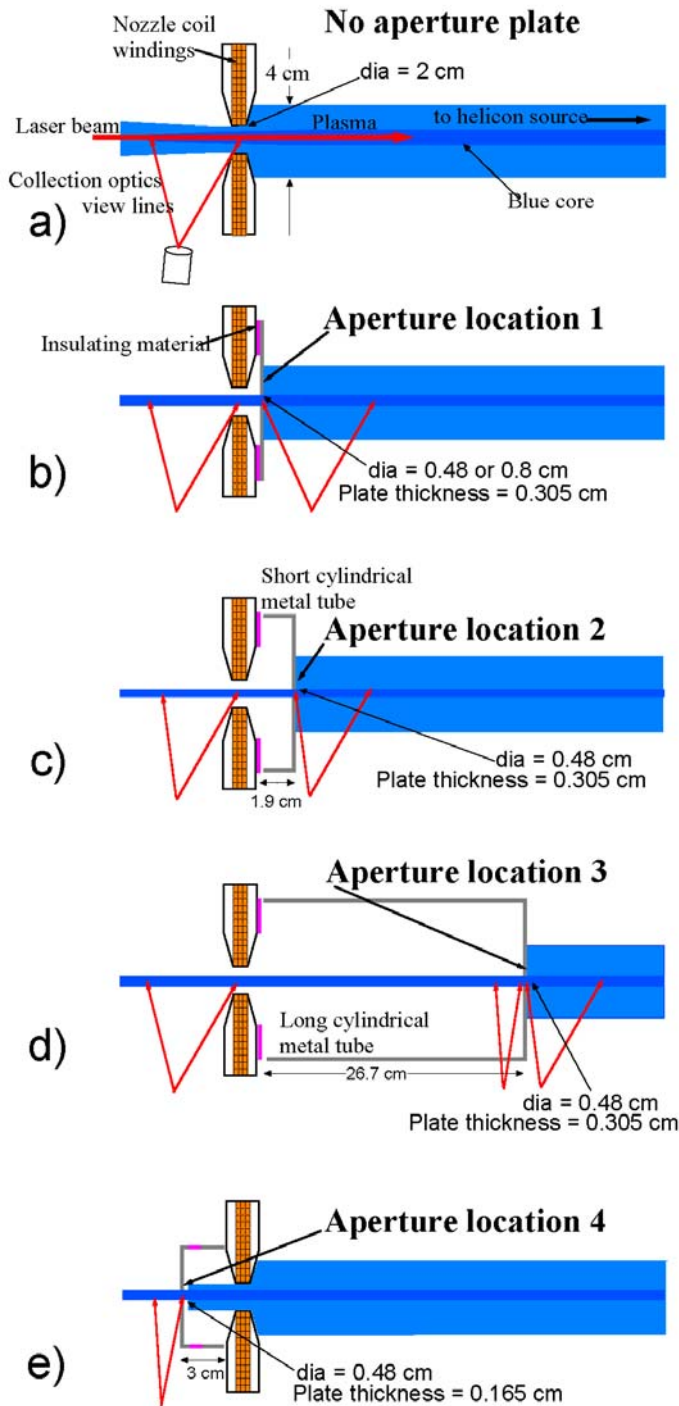
Fig. 7: AP at $z = -29.4$ cm and plasma conditions of $P = 800$ W; $B_M = 580$ G; $B_N = 1100$ Gauss; $P_M = 0.51$ mTorr; $P_{ERB} = 0.11$ mTorr. For measurements in main chamber, the nozzle magnetic field strength was decreased to 200 Gauss. The open diamonds, open circles, and solid circles denote the parallel kinetic energy of LEP, HEP, and SHEP. The SHEP (Super-High-Energy-Population) label identifies ions in the nozzle region that are stationary in source and believed to have passed through two DLs.

Fig. 8: The ion beam energy in the presheath for rf powers of 500 (solid circles), 800 (solid squares) and 1100 (solid diamonds) Watts. $B_H = 580$ G and $P_M = 0.5$ mTorr. Aperture plate at $z = -29.4$ cm (right surface).

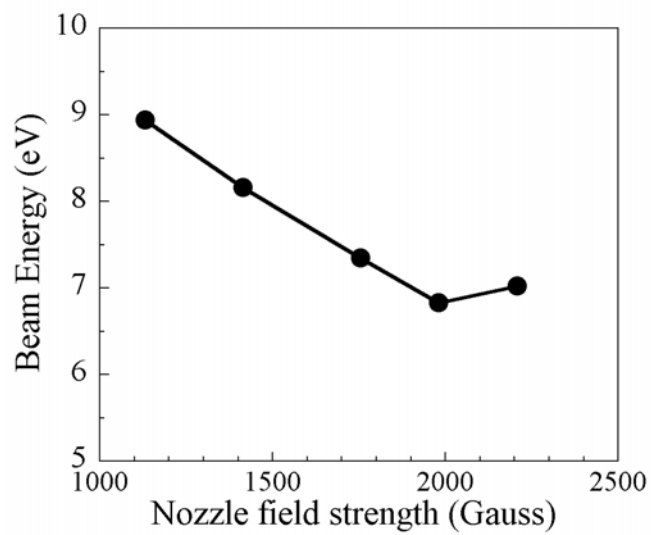
Fig. 9: The ion beam energy (solid circles) at $z = 14.8$ cm and absolute value of aperture plate floating potential (solid squares) versus the nozzle field strength for rf power of 720-850 W, $B_H = 580$ G, $P_M = 0.5$ mTorr, and $P_{ER} = 0.12-0.24$ mTorr. The aperture plate was at $z = 14.0$ cm (left surface) in the ER.



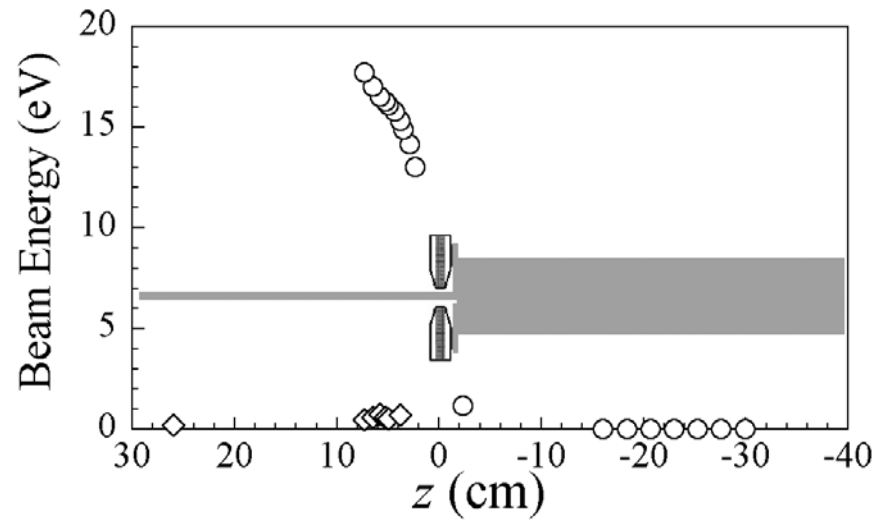
Sun et al. **Fig. 1**



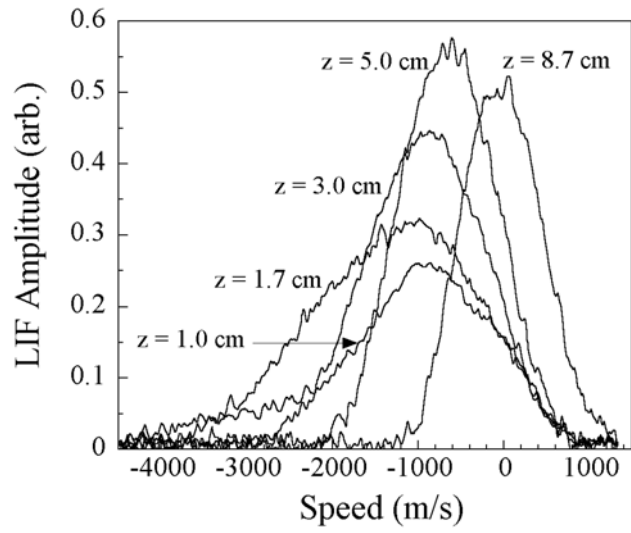
Sun et al. Fig. 2



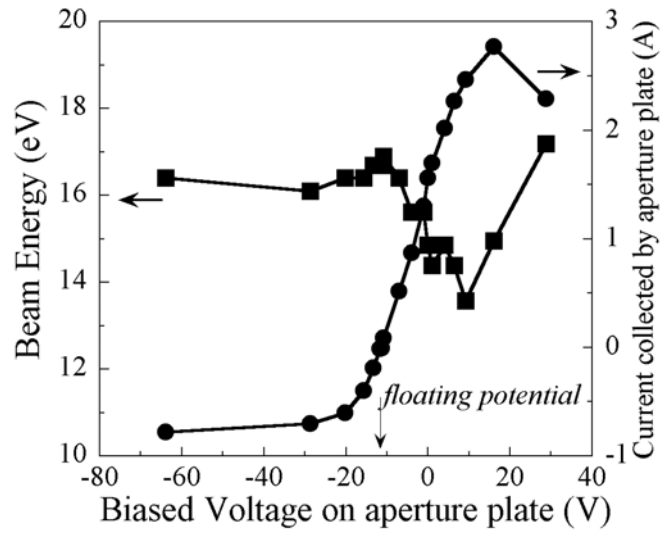
Sun et al. **Fig. 3**



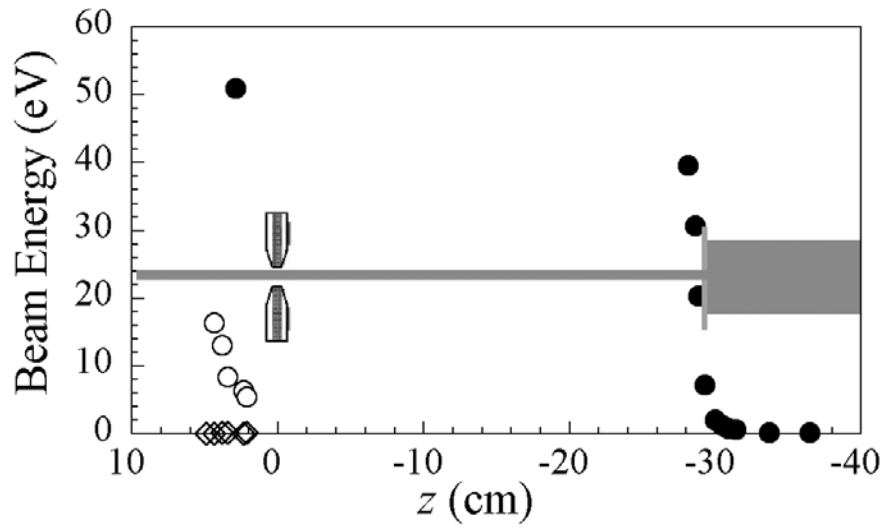
Sun et al. **Fig. 4**



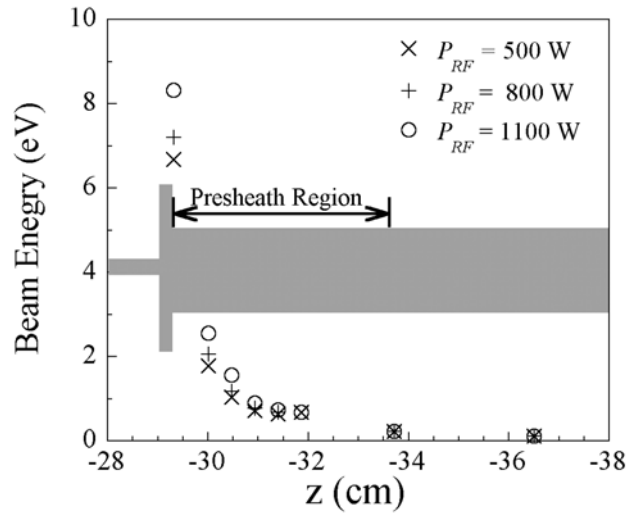
Sun et al. Fig. 5



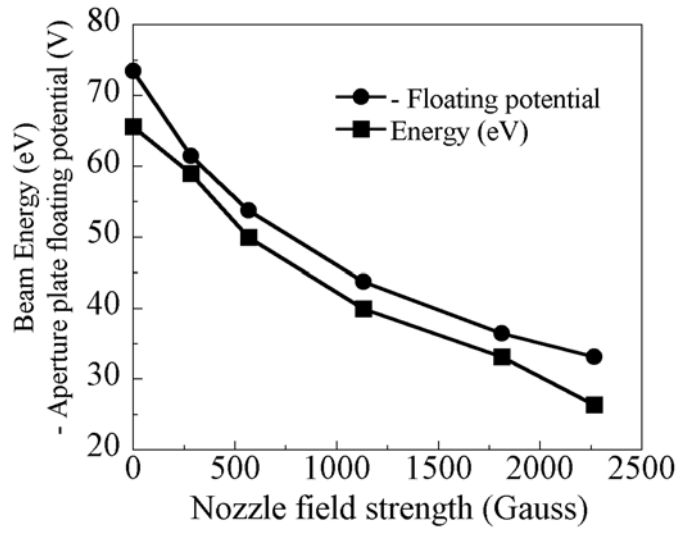
Sun et al. **Fig. 6**



Sun et al. Fig. 7



Sun et al. **Fig. 8**



Sun et al. **Fig. 9**

External Distribution

Plasma Research Laboratory, Australian National University, Australia
Professor I.R. Jones, Flinders University, Australia
Professor João Canalle, Instituto de Fisica DEQ/IF - UERJ, Brazil
Mr. Gerson O. Ludwig, Instituto Nacional de Pesquisas, Brazil
Dr. P.H. Sakanaka, Instituto Fisica, Brazil
The Librarian, Culham Science Center, England
Mrs. S.A. Hutchinson, JET Library, England
Professor M.N. Bussac, Ecole Polytechnique, France
Librarian, Max-Planck-Institut für Plasmaphysik, Germany
Jolan Moldvai, Reports Library, Hungarian Academy of Sciences, Central Research
Institute for Physics, Hungary
Dr. P. Kaw, Institute for Plasma Research, India
Ms. P.J. Pathak, Librarian, Institute for Plasma Research, India
Dr. Pandji Triadyaksa, Fakultas MIPA Universitas Diponegoro, Indonesia
Professor Sami Cuperman, Plasma Physics Group, Tel Aviv University, Israel
Ms. Clelia De Palo, Associazione EURATOM-ENEA, Italy
Dr. G. Grosso, Instituto di Fisica del Plasma, Italy
Librarian, Naka Fusion Research Establishment, JAERI, Japan
Library, Laboratory for Complex Energy Processes, Institute for Advanced Study,
Kyoto University, Japan
Research Information Center, National Institute for Fusion Science, Japan
Professor Toshitaka Idehara, Director, Research Center for Development of Far-Infrared Region,
Fukui University, Japan
Dr. O. Mitarai, Kyushu Tokai University, Japan
Mr. Adefila Olumide, Ilorin, Kwara State, Nigeria
Dr. Jiangang Li, Institute of Plasma Physics, Chinese Academy of Sciences, People's Republic of China
Professor Yuping Huo, School of Physical Science and Technology, People's Republic of China
Library, Academia Sinica, Institute of Plasma Physics, People's Republic of China
Librarian, Institute of Physics, Chinese Academy of Sciences, People's Republic of China
Dr. S. Mirnov, TRINITI, Troitsk, Russian Federation, Russia
Dr. V.S. Strelkov, Kurchatov Institute, Russian Federation, Russia
Kazi Firoz, UPJS, Kosice, Slovakia
Professor Peter Lukac, Katedra Fyziky Plazmy MFF UK, Mlynska dolina F-2, Komenskeho Univerzita,
SK-842 15 Bratislava, Slovakia
Dr. G.S. Lee, Korea Basic Science Institute, South Korea
Dr. Rasulkhozha S. Sharafiddinov, Theoretical Physics Division, Institute of Nuclear Physics, Uzbekistan
Institute for Plasma Research, University of Maryland, USA
Librarian, Fusion Energy Division, Oak Ridge National Laboratory, USA
Librarian, Institute of Fusion Studies, University of Texas, USA
Librarian, Magnetic Fusion Program, Lawrence Livermore National Laboratory, USA
Library, General Atomics, USA
Plasma Physics Group, Fusion Energy Research Program, University of California at San Diego, USA
Plasma Physics Library, Columbia University, USA
Alkesh Punjabi, Center for Fusion Research and Training, Hampton University, USA
Dr. W.M. Stacey, Fusion Research Center, Georgia Institute of Technology, USA
Director, Research Division, OFES, Washington, D.C. 20585-1290

The Princeton Plasma Physics Laboratory is operated
by Princeton University under contract
with the U.S. Department of Energy.

Information Services
Princeton Plasma Physics Laboratory
P.O. Box 451
Princeton, NJ 08543

Phone: 609-243-2750
Fax: 609-243-2751
e-mail: pppl_info@pppl.gov
Internet Address: <http://www.pppl.gov>